Confined fluid between two walls: The case of micelles inside a soap film

Oleg Krichevsky and Joel Stavans
Department of Physics of Complex Systems, Weizmann Institute of Science, Rehovot 76100, Israel
(Received 16 December 1996)

We study by light scattering methods the behavior of soap films drawn from solutions of different surfactant concentration. For concentrations just above the critical micelle concentration, micelles induce a depletion attraction and thus a reduction in equilibrium film thickness. For larger surfactant concentrations we observe stepwise thinning, due to the organization of micelles in layers parallel to the film plane. Our results show that the behavior of the micelles in the confining geometry of the film is analogous to that of ordinary fluids confined between walls. The ability to go from a gaslike to a liquidlike configuration of micelles by changing surfactant concentration allows us to test model predictions of density oscillations in confined liquids. [S1063-651X(97)08206-8]

PACS number(s): 68.15.+e, 61.20.−p

I. INTRODUCTION

Soap films are fascinating objects that have attracted the attention of scientists and laymen alike for centuries. Their peculiar behavior has been the subject of scientific scrutiny since the times of Newton and Hooke, who already noted the interference colors shown by films as they drain, and the black spots appearing during the advanced stages of this process [1,2]. The black spots were identified as corresponding to two possible long-lived states, commonly referred to as the *common* and the *Newton* black films. While common black films have typical thicknesses of a few hundred angstroms, Newton black films are much thinner, reaching thicknesses as small as 40 Å. This behavior was rationalized for a long time in terms of a simple model architecture according to which soap films consist of two monolayers of amphiphilic molecules sandwiching a layer of water. In the case of ionic surfactants, the behavior of such a model film is determined by the competition of repulsive screened Coulomb forces due to the dissociation of ions from the amphiphilic molecules, and attractive Van der Waals forces, both of which comprise the celebrated DLVO potential after Derjagin, Landau, Vervey, and Overbeck [3]. This competition usually results in a minimum of the DLVO potential, and a barrier that prevents the film from falling into a deeper minimum at small distances as shown schematically in Fig. 1. For low ionic content, the barrier is many times larger than k_BT and the common black film associated with it is very stable. However, a transition to the inner minimum identified with the Newton black film can be observed either by fast evaporation of the water core, or by the addition of electrolytes, which screen further the electrostatic repulsion. In this state, the film consists essentially of the two surfactant monolayers separated by a thin hydration layer a few water molecules thick. No further reduction in thickness is possible, and therefore a nearly hard-core repulsion shown in Fig. 1 results.

While the DLVO potential and the model architecture described above may provide an appropriate description of the behavior of films drawn out of solutions with surfactant concentration c below the critical micelle concentration c_{cmc}, recent investigations have revealed that this picture is far from adequate for films drawn out solutions with $c \gg c_{cmc}$. Films drawn from these solutions exhibit a striking stratification phenomenon whereby the film thickness decays in steps of equal height as they drain [4–6]. Within each step the film thickness is nearly time independent, varying by just a few angstroms. Clearly, the existence of more metastable states beyond the common and Newton black films cannot be accounted for by the DLVO model and the behavior must correspond to the presence of more than two minima in the interaction potential $V(h)$ between the two monolayers comprising the film walls. Film stratification has been attributed to the formation of layers of micelles within the aqueous core of the film parallel to the film plane, whose presence had been overlooked in previous theoretical descriptions. In this picture, the observation of a step in thickness corresponds to the expulsion of a micellar layer to the bulk solution the film is in contact with, while the long-lived metastable states correspond to states in which the number of

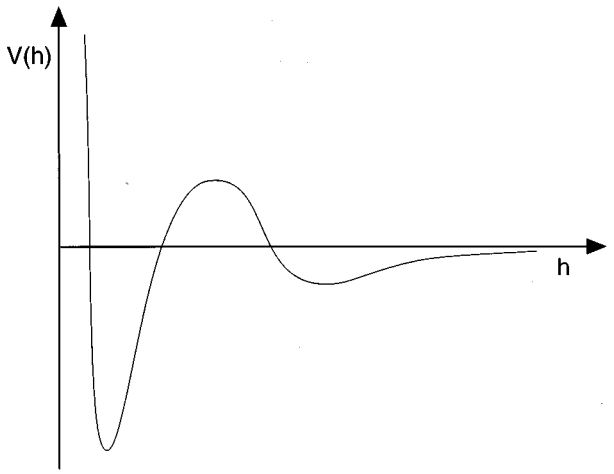

FIG. 1. Typical shape of the DLVO potential as a function of distance. The outer minimum corresponds to the common black film while the inner minimum corresponds to the Newton black film. The steep repulsion at very small distances corresponds to a nearly hard core repulsive interaction between the hydrated monolayers comprising the film walls.

micellar layers is in registry with the film thickness. There is by now considerable evidence supporting this scenario. Direct measurements of the disjoining pressure of stratified films [5], and measurements of forces between two mica plates immersed in a micellar solution using the surface force apparatus technique [7] have revealed an oscillating component in the interaction between the monolayers, which becomes appreciable only when the thickness h is sufficiently small, and whose amplitude decays with increasing h. These findings strongly suggested an analogy between the behavior of stratified films and that of ordinary fluids confined between two hard walls, for which an oscillatory force component termed *structural force* is also observed [8]. In this latter case, the oscillation period corresponds very nearly to the molecular diameter. Our light scattering studies of stratified soap films [6] have supported this analogy, and showed convincingly that liquid state theory models of inhomogeneous liquids can account quantitatively for micellar stratification, the micelles now regarded as a supermolecular fluid. Finally we note that stratification has also been observed in films seeded with solid particles [9].

We have extended our light scattering investigations of free-standing soap films to the case of films drawn out of solutions with c close to but above the c_{cmc}, and in this paper we present the results. Our data clearly show that the DLVO picture is not adequate in this regime either, and that additional attractive interactions such as the depletion forces induced by micelles must be invoked to account for the discrepancy between the observed equilibrium thickness and that predicted by the DLVO potential. Furthermore, we present results on the effects on stratification of screening further the repulsive screened Coulomb interaction by the addition of electrolytes.

II. EXPERIMENTAL METHODS AND MATERIALS

The use of light scattering methods for studying films rests upon the fact that thermally induced corrugations of the surface monolayers scatter light in off-specular directions [10]. For corrugation wavelengths (amplitudes) much larger (smaller) than the film thickness, it can be shown that these corrugations can be decomposed into bending modes in which both monolayers oscillate in phase, and squeezing modes in which the monolayers oscillate with a 180° phase difference. While the former are underdamped and of high typical frequency (they can reach frequencies in the MHz range in the thickness regime in which our experiments are performed), the latter are underdamped, have typical frequencies in the kHz range, and due to the thickness modulations, depend on the interaction potential between the monolayers. The very different typical frequencies of these modes allows for their easy separation in a light scattering measurement.

In our experiments we have used both static and dynamic light scattering (SLS and DLS, respectively) to probe the dynamics of squeezing modes as films drain, and specular reflectivity to determine the instantaneous film thickness. Scattered light from an argon laser ($\lambda = 4880$ Å) was detected by a photomultiplier, whose output was connected either to a counter to obtain the scattered light intensity, or to a correlator to compute its temporal correlation function. The light reflected specularly was detected by means of a photodiode. The scattered intensity of modes of wave vector k is given by [10]

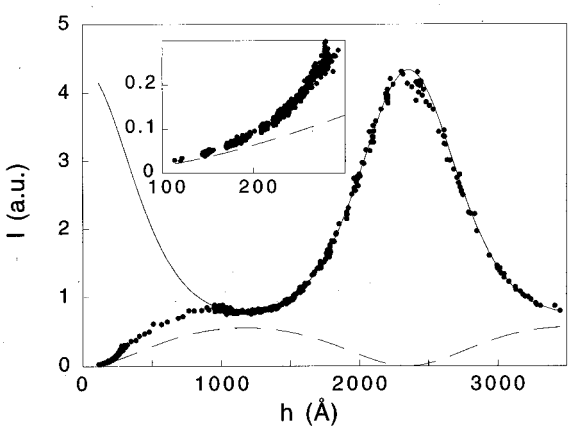

FIG. 2. Scattered intensity $I(h)$ as a function of film thickness h for a film drawn from a solution with $c = 4$ and 4 wt % glycerol. The solid line is a fit with Eq. (1) taking $V''(h) = 0$, while the dashed line denotes the contribution of bending modes only. The inset is an enlargement of the small-h part of the data.

$$I(h,k) = A\left[G_0 G_3 + \frac{2G_1 G_0 - G_0 G_3}{1 + 2V''(h)/\sigma k^2} \right], \tag{1}$$

where σ is the surface tension, $V''(h)$ the second derivative of the interaction potential with respect to h, and the G_i are h-dependent geometric factors defined in Ref. [10], which depend also on the refraction index and the scattering geometry. A is a multiplicative factor found from a fit to the data. The first and second terms in brackets are the contributions from the bending and squeezing modes, respectively. Since all quantities can be measured independently and the only unknown is $V''(h)$, the difference between the values of $I(k,h)$ with $V''(h) = 0$ and the actual data determines $V''(h)$ [11].

We illustrate the method in Fig. 2, where we plot the total scattered intensity $I(h)$ as a function of thickness h for a film drawn from a solution with $c = 4$ wt % [in the following we omit the k dependence of $I(k,h)$ since all our experiments were conducted with the same value of the wave vector: $k \sim 5500\ \mathrm{cm}^{-1}$]. The solid line is a fit of Eq. (1) with $V'' = 0$ to the large-h portion of the data, for which the contribution of the potential is negligible. The dashed line is the calculated contribution of the bending mode. Deviations from the fit, evident below 1000 Å, signal a significant contribution from the potential. The data show that for small h, the contribution to the total scattering from squeezing modes decreases with h, and the contribution from bending modes becomes more dominant. This is more evident in the blowup of the small-h portion of the data shown in the inset. Since the calculation of $V''(h)$ involves a subtraction of the calculated bending mode contribution from the measured data points, the error in the determination of $V''(h)$ for very small h becomes large.

Alternatively, $V''(h)$ can be measured by DLS [10]. In the limit $hk \ll 1$, squeezing modes are overdamped and their characteristic decay time Γ^{-1} is given by

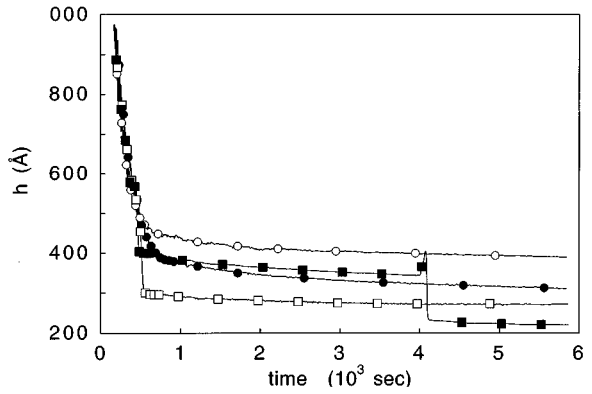

FIG. 3. Thickness h as a function of time t of films drawn out from solutions with different surfactant concentrations: 0.15 (empty circles), 0.25 (full circles), 0.40 (empty squares), and 0.8 (full squares).

$$\Gamma = \frac{\sigma h^3 k^4}{24\eta}\left[1+\frac{2V''(h)}{\sigma k^2}\right], \tag{2}$$

where η is the viscosity. Even though this dispersion relation was derived having in mind a film core devoid of micelles, results previously published demonstrate the consistency between SLS and DLS measurements in the case of stratified films, and the validity of Eq. (2) [6].

Films were drawn out of surfactant solutions by dipping rectangular $0.3\times 2.0\text{-cm}^2$ PVC frames in a Teflon container inside a sealed chamber, where temperature and humidity were kept constant. The temperature of the chamber was kept constant at 20 °C with a precision of ± 0.02 °C. The films were drawn out 12 h after the solutions were introduced into the sealed chamber. Surfactant solutions of different concentrations were prepared from deionized water, glycerol (4 wt %) and sodium dodecyl sulfate, an anionic surfactant purchased from Sigma with a purity of 99%.

III. RESULTS

A. Small surfactant concentrations

The typical draining behavior of films is illustrated in Fig. 3, where we plot the film thickness as a function of time for different values of c around the c_{cmc}. The approach to the equilibrium state is smooth and monotonic for $c = 0.15$ wt %, a concentration below the c_{cmc} (0.23 wt %). This behavior persists when c is increased slightly above the c_{cmc} (0.25 and 0.4 wt %), but notice that the equilibrium film thickness $h_{\rm eq}$ decreases as c is increased. While one may conjecture that the reduction in $h_{\rm eq}$ may be due to the increase in the electrostatic screening effected by the increase in surfactant concentration, two independent measurements of the c dependence of the Debye screening constant κ_D rule this out. In the first measurement, κ_D was extracted from fits to $V''(h)$ for $h<h_{\rm eq}$, in which case the potential is expected to be dominated by the screened Coulomb repulsion. To measure $V''(h)$ in this regime, we reduced gently the humidity in the sealed chamber enclosing the film below its saturation value with a gentle flush of nitrogen. This induced a slow evaporation of the film core resulting in values of the thickness below $h_{\rm eq}$. After the nitrogen flush, the humidity slowly relaxed back to its saturation value and the film thickness increased back to $h_{\rm eq}$. During this slow relaxation, measurements of the scattered intensity were performed from which $V''(h)$ was extracted. $V''(h)$ is shown in Fig. 4 for three different concentrations, together with the contribution of the Van der Waals attraction as calculated by Donners *et al.* [12]. To an excellent approximation, $V''(h)$ decays exponentially in this regime of film thickness while the contribution from the Van der Waals attraction is between one and two orders of magnitude smaller. As expected, the interaction potential is dominated by the electrostatic contribution in this range of h, and we therefore fit the screened Coulomb function $B\exp(-\kappa_D h)$ to our data to extract κ_D. We also obtained κ_D from measurements of the electrical conductivity of our solutions [11]. We show the values of κ_D obtained in these two independent ways in Table I. Both sets of data agree well. Introducing the values of $B\exp(-\kappa_D h)$ obtained from the fit into the DLVO potential yields values of $h_{\rm eq}(c)$ that are much higher than the observed ones (ca. 100 Å). Thus the increase in screening is not enough to account for the reduction in $h_{\rm eq}$ and therefore an additional attractive interaction between the monolayers bounding the film must be involved. The latter can only be of capillary, gravitational, and entropic origin. The first two contributions can be estimated from the balance of forces at $h=h_{\rm eq}(c)$ for films with $c<c_{cmc}$. Subtracting these, one is left with the entropic contribution.

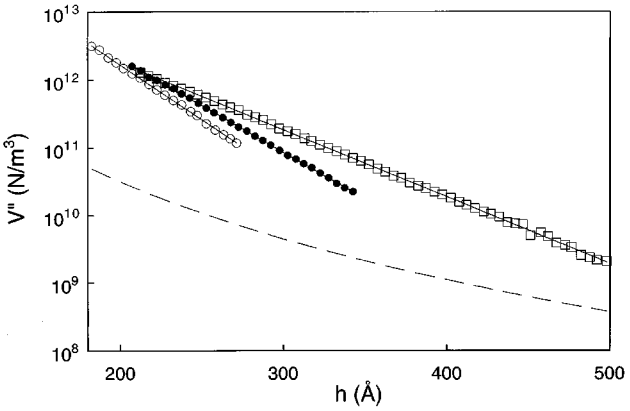

FIG. 4. Second derivative of the interaction potential $V''(h)$ between the monolayers comprising a film for different surfactant concentrations: 0.15 (empty squares), 0.25 (full circles), and 0.40 wt % (empty circles). Solid lines are exponential fits while the dashed line is the calculated Van der Waals contribution. For details see text.

TABLE I. Values of the inverse Debye screening length κ_D obtained from static light scattering (SLS) and conductivity measurements, for different surfactant concentrations c.

c (wt %)	κ_D (nm^{-1}) SLS	κ_D (nm^{-1}) Conductivity
0.15	0.23±0.01	0.24±0.02
0.25	0.31±0.01	0.30±0.02
0.4	0.30±0.01	0.31±0.02
0.8	0.34±0.02	0.36±0.02

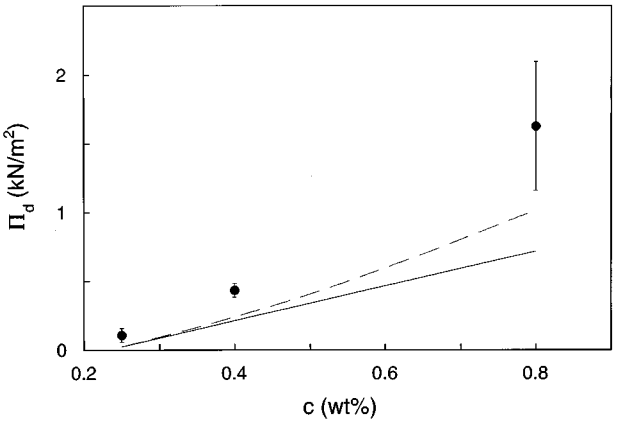

FIG. 5. Depletion attractive force Π_d as a function of surfactant concentration. Solid and dashed lines show the osmotic pressure of an ideal gas of micelles and a gas of interacting micelles, respectively.

In Fig. 5 we show the results of this procedure. We also plot the osmotic pressure due to the micelles Π_d calculated assuming that they constitute an ideal gas (full line), and including intermicellar correlations (dashed line). The latter was calculated using the thermodynamic relation

$$\Pi_d = nk_BT - \frac{2}{3}n^2\int_0^\infty u'_{sc}g(r)r^3dr,$$

where $g(r)$ is the micelle pair correlation function, which we calculated using the rescaled mean spherical approximation (RMSA) [13], a closure scheme known to give an accurate description of fluids interacting via a screened Coulomb potential $u_{sc}(r)$. As inputs to this calculation we used values of the micellar radius and aggregation number as determined experimentally from x-ray investigations [14], and the micellar charge and Debye screening length deduced from the aggregation number and electrical conductivity measurements [11]. The theoretical prediction of the depletion force including the intermicellar interaction provides a much closer approximation to the experimental data than the ideal contribution alone, although it is consistently below the data. We conjecture that an additional osmotic pressure exerted by all the ionic species through the Donnan effect [15] may be responsible for the remaining discrepancy, although we have not made any measurements of ionic concentrations inside the film to prove this.

B. Intermediate and large surfactant concentrations

Returning to Fig. 3, an increase in c to 0.8 wt % brings about a qualitative change in film behavior: instead of reaching its final equilibrium state smoothly, the film passes first through a metastable state of larger thickness. Within this state, the film thickness is nearly time independent and changes by a few angstoms if observed at a higher resolution. The thickness of both the intermediate and final states is reproducible from run to run, although the lifetime of the metastable state may vary, typically increasing with c within a certain range. Notice that keeping with the trend observed in Fig. 3, the thickness of the final equilibrium state is smaller than for smaller values of c.

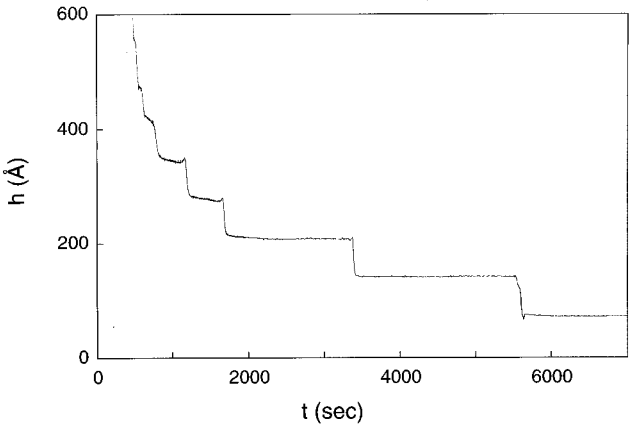

FIG. 6. Thickness h vs time t of a film drawn from a solution with $c=12$ wt %.

As c is increased even further, there is a tendency for more steps to appear, although their number eventually saturates. Large-thickness steps may sometimes be skipped. We have not been able to observe more than 8–9 steps even in films drawn from solutions with $c=16$ wt %. As an example, we show in Fig. 6 the thickness versus time of a draining film corresponding to $c=12$ wt %. Seven steps of equal height (nearly 70 Å) can clearly be discerned. As before, the thickness of each metastable state is nearly time independent and the lifetime of each state varies from run to run. Transitions between succesive states are sometimes preceded by large fluctuations in the scattered intensity, whose time scale is about 5–7 decades slower than the typical time scales of bending and squeezing modes (μsec and msec, respectively). The origin of these large fluctuations is the passing of a rim of liquid separating two metastable states.

In contrast to the number of steps, the step height δ decreases reproducibly with increasing c. This is clearly seen in the change in slope in plots of the thickness of metastable states for different surfactant concentrations as shown in Fig. 7. A plot of δ versus c has been published elsewhere [6]. This decrease reflects mainly the decrease in the intermicel-

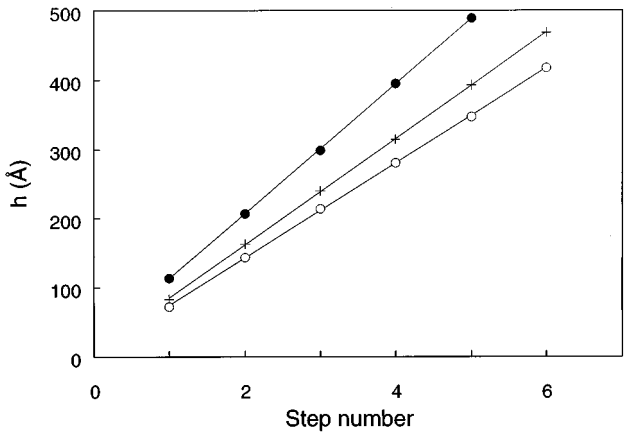

FIG. 7. Thickness of metastable states h vs step number for $c=4$ (full circles), 8 (crosses), and 12 wt % (empty circles). Error bars are smaller than the data symbols. Straight lines are linear fits to the data.

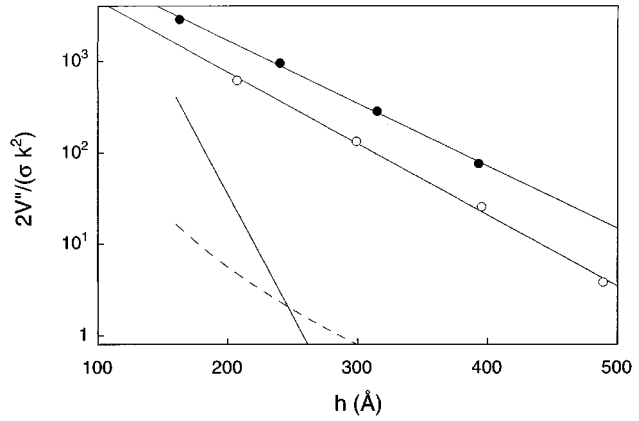

FIG. 8. Second derivative of the interaction potential $V''(h)$ as a function of film thickness h for c: 4 (empty circles) and 8 wt % (full circles). Also shown are the contributions from the screened Coulomb (full line) and Van der Waals (dashed line) forces.

lar distance. For all values of c, δ is larger than the micellar hard core diameter (46 ± 2 Å) [14], although the data approach this value asymptotically.

We have studied the change in the behavior of $V''(h)$ for large surfactant concentrations. The dependence of $V''(h)$ on h measured at thick metastable states is shown in Fig. 8 for two surfactant concentrations, together with the contributions of the electrostatic and Van der Waals forces. The proximity of the data points of $I(h)$ to the bending mode contribution for small h precluded the calculation of $V''(h)$ for metastable states of small thickness. To a very good approximation $V''(h)$ and consequently $V(h)$ decay exponentially. We stress that even though this *structural force* and the screened electrostatic interaction both decay exponentially with distance, they behave very differently when c is varied. The characteristic decay length ζ of the structural force is plotted in Fig. 9 for different surfactant concentrations. The large error bars at large c are again due to the uncertainty in the measurement of $V''(h)$ for small values of h. Notice that ζ increases with the micellar volume fraction, which is consistent with the increase in the number of metastable states with increasing c. In contrast, κ_D^{-1}, which is much smaller than ζ, decreases with c: while $\kappa_D^{-1}=31$ Å for $c=0.5$ wt %, it is nearly 8 Å for $c=16$ wt %. Thus structural forces provide the dominant contribution to the repulsive interactions stabilizing metastable states.

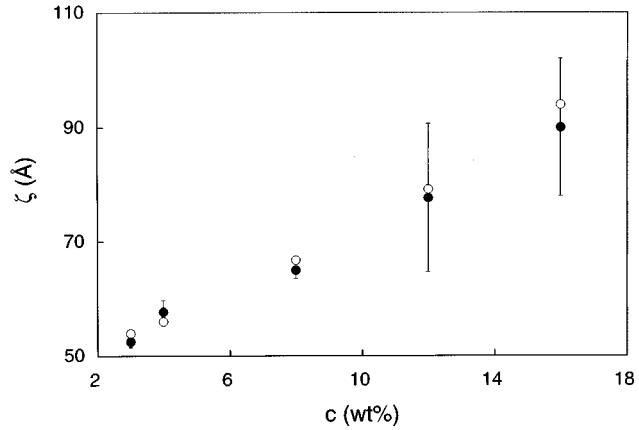

FIG. 9. Characteristic decay length ζ of the interaction potential as a function of surfactant concentration c. Full circles: experimental results, error bars denoting one standard deviation from measurements on three different films. Empty circles: theoretical results from the RMSA calculation.

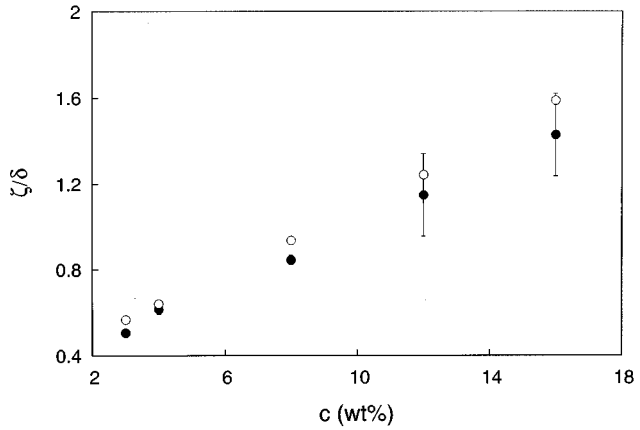

FIG. 10. Ratio of the decay length of the structural force ζ to the step height δ as a function of the surfactant concentration c: experimental (full circles) and theoretical (empty circles) results. For details see text.

The behavior we observe for large values of c shares many features in common with that displayed by confined liquids. Both the exponential decay of $V(h)$ due to the structural force, and the dominance of the latter over other interactions present is also observed when ordinary fluids are confined between the solid walls of a surface force apparatus [8]. To make a more quantitative comparison between real liquids and the micellar supermolecular fluid within a film, it is useful to define the nondimensional parameter ζ/δ. As shown in Fig. 10, ζ/δ increases with c, from about 0.5 at $c=3$ wt %, to 1.6 at $c=16$ wt %. At the same time, since the screening length κ_D^{-1} decreases, the intermicellar interaction has an increasingly hard core character. Therefore, the values of ζ/δ in this regime should be comparable with those of ordinary fluids, whose structure is dominated by their hard core. This proves indeed to be the case: the range of values observed in fluids falls between 1.2 and 1.7, as with the micellar fluid for $c>12$ wt %.

Given the similarity in behaviors, it is tempting to use theoretical descriptions of confined ordinary liquids to describe the micellar fluid in a film. Various models of the structure of fluids confined between two walls have been proposed [16,17]. Among these, the model by Tarazona and Vicente is simple and its predictions are readily testable with our experimental data. Their model is based on an expansion of the grand potential energy functional $\Omega(\rho)$ of a fluid near a constant value of the bulk density $\rho=\rho_0$. According to the model, the fluid density at a distance z from a wall is given by

$$\rho(z)=\rho_0+Ce^{-ik_0z}e^{-z/\zeta},$$

where C is a constant, k_0 is the wave vector at which the structure factor $S(k)$ of the bulk liquid attains its maximum, and the decay length ζ is given by

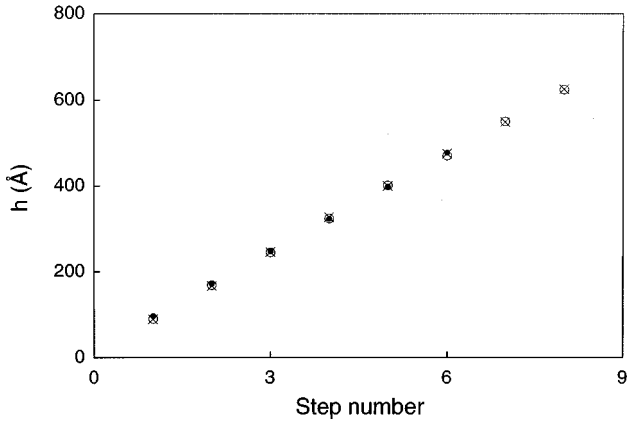

FIG. 11. Step thickness as a function of step number for films with $c=8$ wt % for three different salt (NaCl) concentrations c_s: 0 (empty circles), 10 (crosses), and 20 mM (full circles).

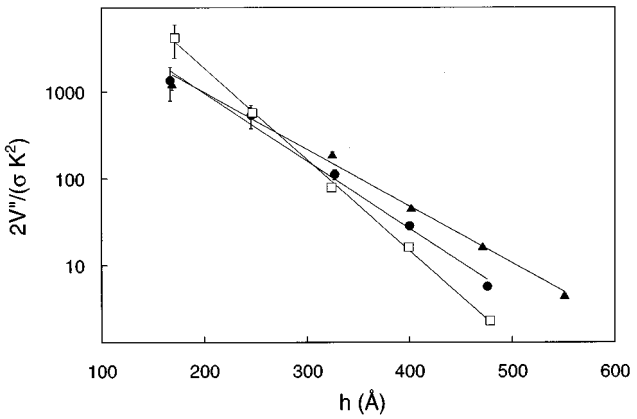

FIG. 12. Normalized second derivative of the interaction potential $2V''(h)/\sigma k^2$ vs thickness h for films with $c=8$ wt % and three different salt (NaCl) concentrations c_s: 0 (triangles), 10 (full circles), and 20 mM (squares).

$$\zeta^{-2}=-\frac{S(k_0)}{S''(k_0)}.$$

In our case, ρ and $S(k)$ refer to the density and structure factor of the micellar fluid. We have not found experimental measurements of $S(k)$ of sufficiently high precision that would allow us to calculate $S(k_0)$ and its curvature at the maximum $S''(k_0)$, and thence ζ. Instead, we have obtained these two parameters from a calculation of $S(k)$ using the RMSA. As inputs to this calculation we have used values of the micellar radius and aggregation number as determined experimentally from x-ray investigations [14], and the micellar charge and Debye screening length deduced from the aggregation number and electrical conductivity measurements. The calculated values of ζ for different values of c shown in Fig. 9 are in good agreeement with our measurements [11]. Quantitative agreement between the predicted values of ζ/δ by the same scheme of calculation and the measured values is also very good (Fig. 10). To compute this ratio, we calculated the pair correlation function from $S(k)$, and deduced from the former the average intermicellar distance in the bulk as a function of c. This estimate is better than that obtained from k_0.

C. The effects of added electrolytes

While changes in c have the effect of changing both the micellar volume fraction and the screening length κ_D^{-1}, one can tune the intermicellar interaction independently by adding electrolytes to the solution. In Fig. 11 we plot the step thickness as a function of step number for films with $c=8$ wt % for three different salt (NaCl) concentrations c_s: 0, 10, and 20 mM in the solution. Within experimental error all the results overlap, showing that in this range of variation of c_s, the thickness of the steps is rather insensitive to the ionic content, and therefore δ is determined primarily by the micellar concentration. It is interesting to note that the addition of 10 and 20 mM of NaCl yields the same value of κ_D^{-1} as the addition of 1.3 and 2.5 wt % of surfactant, respectively. In contrast to the salt, however, these amounts of surfactant do induce a measurable reduction in δ [6]. Another interesting feature of Fig. 11 is that in the case of $c_s=20$ mM, the two thickest steps (steps 7 and 8) have disappeared. More and more steps disappear as the ionic content of the solution is increased further, and for $c_s>50$ mM no more steps are observed. It is important to note in this context that the micellar size is rather insensitive to ionic content in the regime of c_s of our experiments [18]. Unlike the step height, the potential of interaction between the monolayers $V(h)$ is sensitive to the ionic content. This is clearly demonstrated in Fig. 12 where we plot $V''(h)$ versus h for the same values of c_s as in Fig. 11. As c_s increases, $V''(h)$ decays faster, and hence the value of ζ decreases. Thus the extent of layering penetration into the bulk of a film decreases with increasing salt, a result that is consistent with the disappearance of steps mentioned above. These findings can be rationalized by the fact that our small addition of salt weakens the intermicellar repulsion, and therefore $V(h)$, which depends on it. However, the repulsion is still strong enough to keep micelles away from each other, and thus the intermicellar distance and δ are unaffected. This qualitative picture is supported by our RMSA calculations. An additional reduction of the potential may arise from the Donnan effect [15].

IV. CONCLUSIONS

Our studies show conclusively that free-standing soap films stabilized by ionic surfactants cannot be described by taking into account only electrostatic and Van der Waals forces. When a film is drawn out of a solution with $c \geqslant c_{cmc}$, the micelles within the film core induce depletion and structural forces that contribute significantly to the behavior of a film. Our findings underscore the strong similarities between the behavior of the supermolecular fluid of micelles in the film and that exhibited by ordinary fluids confined between two walls. Furthermore, the analysis of our data shows that models tailored for the latter can also describe quantitatively the behavior of the former. In fact, in the case of large surfactant concentrations for which the micellar volume fraction is sufficiently high, the intermicellar interactions are strongly screened and therefore more hard-core-like; the values of the nondimensional ratio ζ/δ we measure and calculate are comparable to those observed in ex-

periments on ordinary fluids in a surface force apparatus. While increasing the surfactant concentration also had the effect of changing the screening of the electrostatic force between micelles, we were able to tune the latter independently by varying the ionic content of our solutions. Our results show that the step height is not affected by the addition of electrolytes and is therefore determined by the micellar volume fraction in the regime of concentrations we used. Unlike the step height, structural forces are very sensitive to the ionic content and small additions of salt induce a significant decrease in ζ and the disappearance of steps of large thickness.

As a final note, we stress that the ability to make a large sweep in micellar volume fraction was critical to our experiments. This stands in contrast to ordinary fluids, for which analogous measurements over a large range of densities have never been performed. In light of this study, it would be very interesting to use light scattering techniques to study films stabilized by nonionic surfactants, for which stratification has already been observed [19]. We plan to perform these experiments in the near future.

ACKNOWLEDGMENTS

We thank Ch. Ligoure for bringing Ref. [15] to our attention. This study was supported by the Minerva Foundation (J.S.).

[1] I. Newton, *Optiks* (Smith and Walford, London, 1704); R. Hooke, in *The History of the Royal Society of London* (T. Birch, London, 1757).

[2] E. S. Johonnott, Philos. Mag. **11**, 746 (1906); J. Perrin, Ann. Phys. (Leipzig) **10**, 160 (1918).

[3] B. V. Derjaguin and L. D. Landau, Acta Physicochim. URSS **14**, 633 (1941); E. J. W. Verwey and J. Th. G. Overbeek, *Theory of the Stability of Lyophobic Colloids* (Elsevier, Amsterdam, 1948).

[4] A. D. Nikolov and D. T. Wasan, J. Colloid Interface Sci. **133**, 1 (1989); M. N. Jones, K. J. Mysels, and P. C. Scholten, Trans. Faraday Soc. **62**, 1336 (1966); A. Sonin and D. Langevin, Europhys. Lett. **22**, 271 (1993); A. D. Nikolov, D. T. Wasan, P. A. Kralchevsky, and I. B. Ivanov, J. Colloid Interface Sci. **133**, 1 (1989); P. A. Kralchevsky, K. D. Danov, and I. B. Ivanov, in *Foams: Theory, Measurements and Applications*, edited by R. K. Prud'homme (M. Dekker, New York, 1995), and references therein.

[5] V. Bergeron and C. J. Radke, Langmuir **8**, 3020 (1992).

[6] O. Krichevsky and J. Stavans, Phys. Rev. Lett. **74**, 2752 (1995).

[7] P. Richetti and P. Kékicheff, Phys. Rev. Lett. **68**, 1951 (1992); J. L. Parker, P. Richetti, P. Kékicheff, and S. Sarman, Phys. Rev. Lett. **68**, 1955 (1992).

[8] J. Israelachvili, *Intermolecular and Surface Forces* (Academic Press, London, 1992).

[9] A. D. Nikolov and D. T. Wasan, Langmuir **8**, 2985 (1992).

[10] C. Y. Young and N. A. Clark, J. Chem. Phys. **74**, 4171 (1981); A. Vrij, J. G. H. Joosten, and H. M. Fijnaut, Adv. Chem. Phys. **48**, 329 (1981), and references therein.

[11] O. Krichevsky, Ph.D. thesis, Weizmann Institute 1995 (unpublished).

[12] W. A. B. Donners, J. B. Rijnbout, and A. Vrij, J. Colloid Interface Sci. **60**, 540 (1977).

[13] J. B. Hayter and J. Penfold, Mol. Phys. **42**, 109 (1981); J. B. Hayter and J. Penfold (unpublished); J. P. Hansen and I. R. McDonald, *Theory of Simple Fluids* (Academic, New York, 1986).

[14] F. Reiss-Husson and V. Luzzati, J. Phys. Chem. **68**, 3504 (1964).

[15] M. Dubois, Th. Zemb, L. Belloni, A. Delville, P. Levitz, and R. Setton, J. Chem. Phys. **96**, 2278 (1992).

[16] R. Kjellander and S. Sarman, Mol. Phys. **70**, 215 (1990); W. J. van Megen and I. K. Snook, J. Chem. Phys. **74**, 1409 (1981); V. Y. Antonchenko, V. V. Ilyin, N. N. Makovsky, A. N. Pavlov, and V. P. Sokhan, Mol. Phys. **52**, 345 (1984); J. E. Lane and T. H. Spurling, Chem. Phys. Lett. **67**, 107 (1979).

[17] P. Tarazona and L. Vicente, Mol. Phys. **56**, 557 (1985).

[18] M. Corti and V. Degiorgio, J. Phys. Chem. **85**, 711 (1981).

[19] A. D. Nikolov, D. T. Wassan, N. D. Denkov, P. A. Kralchevsky, and I. B. Ivanov, Prog. Colloid Polym. Sci. **82**, 87 (1990).